3D Numerical Modelling of Claw-pole Alternators with its Electrical Environment

Guillaume Caron, Thomas Henneron, Francis Piriou, P Faverolle, J.-C Mipo

3D Numerical Modelling of Claw-pole Alternators with its Electrical Environment

G. Caron[1], T. Henneron[1], F. Piriou[1], P. Faverolle[2], and J.-C. Mipo[2]
[1]Univ. Lille, Arts et Métiers ParisTech, Centrale Lille, HEI, EA 2697 - L2EP - Laboratoire d'Électrotechnique et d'Électronique de Puissance, F-59000 Lille, France.
[2]Valeo Electrical Systems, 94046 Créteil Cedex, France.

This paper describes a methodology for modelling a six-phase claw-pole alternator with its electrical environment. Magnetic nonlinearities, eddy currents and rectifiers are taken into account. To solve magnetodynamic problems, we use the modified magnetic vector potential formulation. The complex structure of the machine requires a 3D finite element analysis. To limit the mesh size, we introduced a refinement strategy based on the calculation of the time derivative of magnetic vector potential, solution of the magnetostatic case. In addition, we propose to reduce the transient state by improving the initial solution from the solution of a magnetostatic problem. These different numerical techniques reduce drastically the computational time and memory resources. To validate the proposed approach, some results are compared with experimental ones.

***Index Terms*—Claw-pole alternator, finite element method, coupling problem**

I. Introduction

THE 3D finite element method combined with a time-stepping method (TSFEM) is classically used to model the claw-pole alternator. This method is popular due to its robustness, accuracy and ease of implementation. In the literature, a large number of papers focus on the modelling of the claw pole machine, but often due to its complexity, assumptions are made. For example, eddy currents are frequently neglected [1], [2] or the electrical environment is replaced by simple electrical circuits [3]. Indeed, to ensure sufficient accuracy of the solution, the mesh needs to be sufficiently fine to preserve details of the rotor geometry and to take into account the eddy currents in the rotor. In the literature, to limit the mesh size, techniques based on mesh refinement have been proposed. Some of them use error estimators [4] to determine areas to refine, while others use indicators computed from the magnetodynamic solution [3]. The optimisation of the mesh limits the number of elements while being adapted to the presence of the eddy currents for a high-rotational speed of the rotor. Moreover, the presence of eddy currents and the electrical environment generate an important transient state which has a huge impact on computational time. This explains the emergence of numerical approaches that compute the steady state directly. Among these, one can deal about the spectral methods [5] which relies on the decomposition of the solution in the Fourier series. Other methods can obtain the steady state directly but in the time domain [6], [7]. Nevertheless, these approaches require to solve very large non-symmetric matrix systems.

This paper focus on a combination of different numerical techniques to model 3D claw-pole alternator taking into account magnetic nonlinearities, eddy currents and rectifiers. Firstly, the 3D model of the claw-pole alternator with its electrical environment composed of two double rectifiers and a battery is presented. Then, an approach to determine an adapted mesh to eddy currents is developed and a technique to reduce the transient state is proposed. Finally, the alternator is modelled at no-load and for different operating points. To validate our model, the results were compared to the experimental ones.

II. 3D model of the alternator

In our study, we consider a ring-shape stator composed of 72 slots provided with two three-phase delta-connected windings, a rotor composed of six claw-pole pairs and magnets to improve the rotor flux path. This latter is generated by an excitation coil arranged coaxially to the claw-pole rotor. The rotational speed of the rotor varies from 1500 to $18000 rpm$. The different parts of the claw-pole alternator are illustrated in Fig. 1. Nevertheless, due to the symmetry of the machine, only a sixth of the studied part can be considered. The rotor and the stator are made with magnetic materials with a nonlinear behaviour. Moreover, as the rotor is massive, his electrical conductivity can't be neglected.

In this context, using the modified magnetic vector potential $\mathbf{A}$ [8], the magnetic problem is described by the equations

$$curl\, \nu(\mathbf{A}) curl\, \mathbf{A} + \sigma \frac{\partial \mathbf{A}}{\partial t} = \sum_{k=1}^{N_{st}} \mathbf{N}_k i_k \tag{1}$$

$$\mathbf{B} = curl\, \mathbf{A} \tag{2}$$

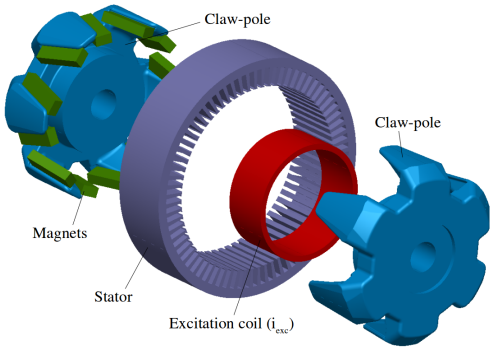

Fig. 1. Exploded view of the claw pole alternator

$$\mathbf{H} = \nu(\mathbf{B})\mathbf{B} \tag{3}$$

with $\mathbf{B}$ the magnetic flux density, $\mathbf{H}$ the magnetic field, ν the reluctivity, σ the conductivity, N_{st} the number of stranded inductors, $\mathbf{N}_k$ the unit current density vector [7] depending on the geometry of the k^{th} winding and i_k its corresponding current. The movement of the rotor is taken into account by the lock-step method [9].

The alternator is simulated in its electrical environment (Fig. 2) namely, the rotor winding is supplied by DC excitation current i_{exc} varying from $1A$ to $5A$. The stator winding is composed of two three-phase systems. The phase shift between the two three-phase systems is 60^o and both systems are connected to a six-pulse diode rectifiers. Electrical circuit equations of the electromagnetic device are obtained from the Kirchoff Voltage Law. Thus, we obtain N_s mesh equations and one of them can be written as

$$U_{bat} = R_k i_k + \frac{d\phi_k}{dt} + V_l + V_m \tag{4}$$

with U_{bat} the battery voltage, R_k the resistance of the coil, ϕ_k the flux linkage of the winding k and, V_l and V_m the voltage across the diodes l and m of a rectifier. The linkage flux can be expressed by the relation $\phi_k = \int \mathbf{A} \cdot \mathbf{N}_k dD$.

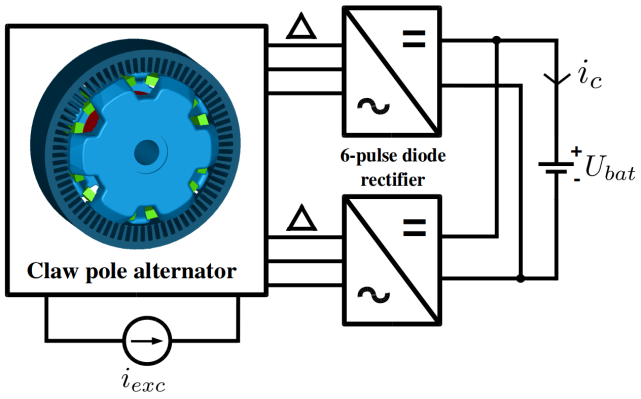

Fig. 2. Claw pole alternator in its electrical environment

III. Numerical techniques

A. Time-stepping finite element method

The time-stepping finite element method is used to discretise (1) and (4). More precisely, it is a combination between the finite element method with the edge elements [10] for the space discretisation and a time-stepping method, namely, the implicit Euler method in our case, for the time discretisation. The coupling between (1) and (4) is obtained by the current i_k and the linkage flux ϕ_k. Under these conditions, the complete equation system to solve at the j^{th} time-step takes the form

$$\begin{cases} \left(\mathbf{M}(\mathcal{A}_j) + \frac{1}{\Delta t}\mathbf{S}\right)\mathcal{A}_j - \mathbf{F}\mathbf{I}_j = \frac{1}{\Delta t}\mathbf{S}\mathcal{A}_{j-1} \\ \mathbf{R}\mathbf{I}_j + \frac{1}{\Delta t}\mathbf{F}^t\mathcal{A}_j = \\ \qquad \frac{1}{\Delta t}\mathbf{F}^t\mathcal{A}_{j-1} - \mathbf{G}\mathbf{\Gamma}_j - \mathbf{U}_j \end{cases} \tag{5}$$

with $\mathcal{A}$ the solution vector of size N_x corresponding to the circulation of the modified magnetic vector potential on all edges of the mesh, Δt the time step, $\mathbf{M}(\mathcal{A}))$ and $\mathbf{S}$ respectively the nonlinear curl-curl and the conductivity matrices of size $N_x \times N_x$, $\mathbf{F}$ a rectangular matrix of size $N_x \times N_s$, $\mathbf{I}$ and $\mathbf{U}$ respectively the current and the voltage vectors of size N_s, $\mathbf{R}$ the resistance diagonal matrices of size $N_s \times N_s$, $\mathbf{\Gamma}$ the vector of size N_s corresponding to the nonlinear forward voltage drop in diodes and $\mathbf{G}$ a state matrix of size $N_s \times N_s$ which depends on diode states in the rectifiers.

B. Adaptive mesh strategy

The modelling of the alternator by the finite element method requires considerable time and memory resources. One of these reasons is due to the number of N_x unknowns depending on the mesh size. Indeed, the mesh must be sufficiently fine to preserve the complex geometry. But more importantly, the mesh of the rotor must be adapted to the presence of eddy currents which can require a huge number of elements.

In this context, a meshing strategy is required to limit the number of elements in the conductive domains of the mesh. Similarly to [3], a refinement approach based on an indicator is used. The idea is to start from a coarse mesh that nevertheless respects the geometry and to refine the areas where the indicator is the highest. These operations can be repeated until the solution obtained on two successive meshes is relatively close to each other.

Our indicator is calculated from the magnitude time variation of the magnetic vector potential of magnetostatic problem. Indeed, the eddy currents appear in the areas where the magnetic induction varies as a function of time and *a fortiori* in the areas where the magnetic vector potential varies as a function of time. In addition, to take into account precisely the variation, our indicator is averaged from the magnitude of the time derivative of the magnetic vector potential over an electrical period. Fig. 3 represents an example of the time derivative of magnetic vector potential obtained from a calculation of the claw pole alternator at no-load. Fig. 4 represents the indicator in the rotor in logarithm scale. As expected, the areas affected by the refinement are located on the top of the claws since they are subjected to the strongest variations of the magnetic flux density. The refinement is achieved with the HOMARD module of SALOME [11] that uses the standard splitting algorithm followed by a second step to manage any non-conforming areas.

In practice, when this algorithm is applied to the claw-pole alternator, the number of elements strongly increases after two iterations of refinement. Indeed, starting from an initial mesh of 313K tetrahedrons in the rotor, we obtain a mesh of 3.35M tetrahedrons after only two iterations.

C. Transient state reduction

Although the mesh is optimised, the computational time can be still important on account of the presence of the transient state. Indeed, having no information on the final state of the system, it is conventional to take a zero initial condition which can lead to a long transient state.

To reduce the transient state and so the computational time, we propose a strategy to evaluate the value of the initial solution. An initial computation is realised when the conductivity of the rotor is neglected until the solution reaches the steady

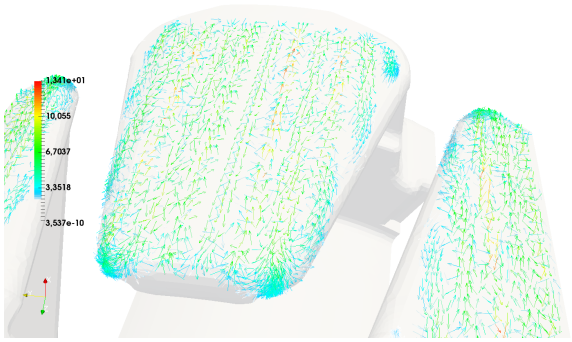

Fig. 3. Time derivative of the magnetic vector potential for a given time-step

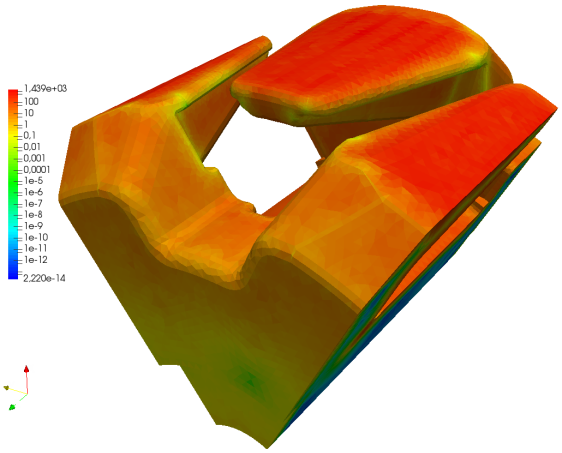

Fig. 4. Indicator of the areas where the variation of the magnetic vector potential is the greatest in the logarithm scale

state. Then, we use this solution as initial condition for the magnetodynamic problem.

In order to validate this approach, we carried out a computation for a given operating point ($6000rpm$, $i_{exc} = 1A$) and we compare the results with those obtained for the magnetodynamic computation with a zero initial condition. Fig. 5 represents the evolution of the rectified current i_c in the battery, we notice that the transient state is relatively short when the eddy currents are neglected. This makes possible to obtain the steady state of magnetodynamic problem in less than 10 electrical periods. Consequently, the computational times are drastically reduced compared to the conventional approach whose steady state is still not reached after $60ms$. Indeed, our approach allows to spend from several days of computational time to only a few hours.

IV. Results

The numerical methods presented in this paper have been implemented in the finite element code of our laboratory: *code_Carmel*[12].

A. Claw-pole alternator with no-load

The discrete problem (5) can easily be adapted to the no-load test. In this case, the numerical technique consisting to reduce the transient state is still available. Considering

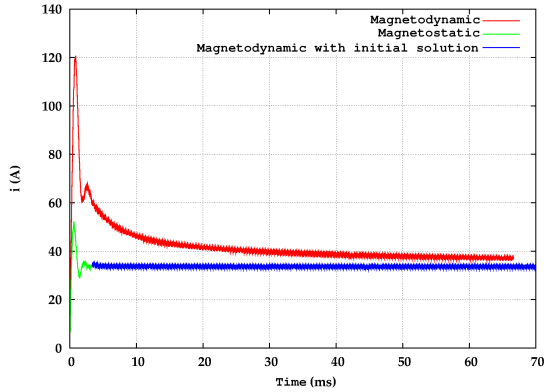

Fig. 5. Rectified current (A) in the battery i_c

an excitation current (i_{exc}) of $3A$ with a rotor speed of $12000rpm$, the emf in the first 3-phases windings at the steady state is shown in Fig. 6. The distribution of the eddy current density is represented in Fig. 7.

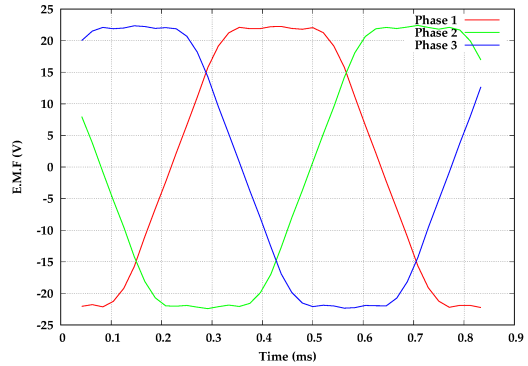

Fig. 6. Emf(V) in the first 3-phases windings at the steady state

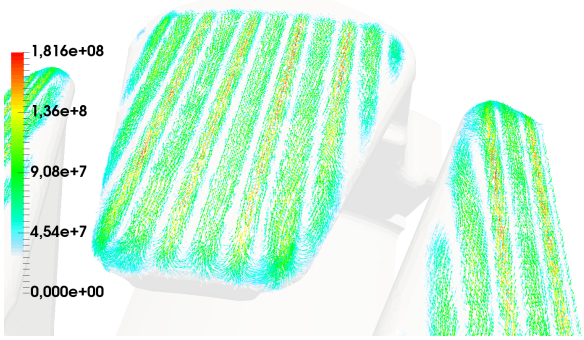

Fig. 7. Eddy current density ($A.m^{-2}$) in the rotor

B. Claw-pole alternator with load

For different operating points, we have compared our results with experimental measurements, and more specifically, the currents in the battery. We performed a parametric study for which we took different values of excitation current and of rotor speed. We present the relative error in percent in the table I. The results show that the error is less than 4% for almost all cases.

To further describe the simulation results, let's take the case where the rotor speed is $12000rpm$ and the excitation current $i_{exc} = 3A$ and the case where the rotor speed is $6000rpm$

and the excitation current $i_{exc} = 5A$. Fig. 8 and Fig. 9 illustrate the steady state currents in the first 3-phases of delta connection. The eddy current density in the rotor obtained for both calculations is shown in Fig. 10 and Fig. 11 for the same time-step.

TABLE I
THE RELATIVE ERROR IN % OF RECTIFIED CURRENT IN THE BATTERY OBTAINED BY OUR MODEL AND COMPARED TO MEASUREMENTS

	1800 rpm	**3000 rpm**	**6000 rpm**	**12000 rpm**	**18000 rpm**
1A			8.04	3.65	3.01
3A	0.69	3.00	3.84	4.01	3.75
5A	4.15	3.02	0.87	2.17	1.45

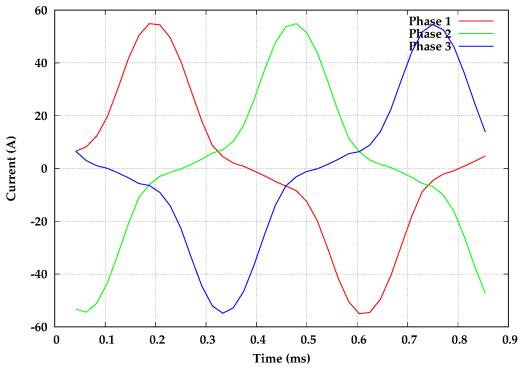

Fig. 8. Currents (A) in the first 3-phase windings at the steady state ($i_{exc} = 3A$, $12000rpm$)

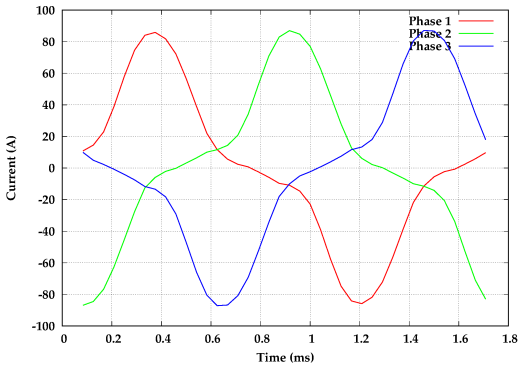

Fig. 9. Currents (A) in the first 3-phase windings at the steady state ($i_{exc} = 5A$, $6000rpm$)

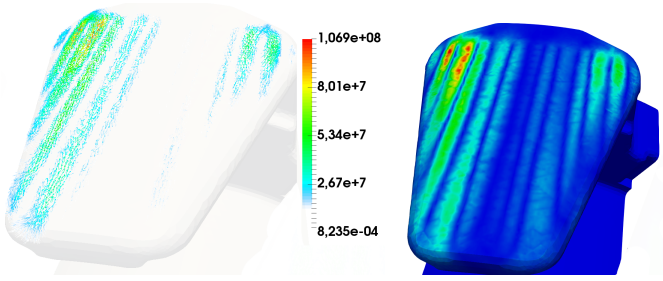

(a) Distribution (b) Module

Fig. 10. Eddy current density ($A.m^{-2}$) at the steady state ($i_{exc} = 3A$, $12000rpm$)

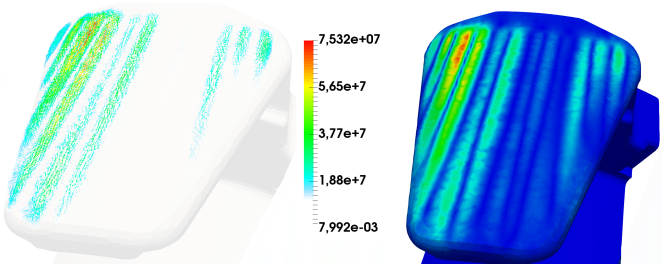

(a) Distribution (b) Module

Fig. 11. Eddy current density ($A.m^{-2}$) at the steady state ($i_{exc} = 5A$, $6000rpm$)

V. CONCLUSION

The purpose of this paper is to model a claw-pole alternator with its electrical environment with acceptable computational time. First, a mesh refinement algorithm is proposed to obtain an optimal mesh adapted to eddy currents. Then, to reduce the transient state, we proposed to carry out a pre-simulation in which the eddy currents in the rotor have been neglected in order to obtain a better initial solution. The numerical results compared to the experimental ones highlight the effectiveness of our model.

REFERENCES

[1] C. Stoica, D. Cazacu, and L. Melcescu, "3d numerical modeling with fem operation under load on the alternator claw poles." in *2015 7th International Conference on Electronics, Computers and Artificial Intelligence (ECAI)*, June 2015, pp. P–75–P–80.

[2] D. Bilyi, V. Bilyi, and D. Gerling, "Fem based model development and co-simulation of automotive multi-phase claw-pole alternator and rectifier," in *2016 IEEE Transportation Electrification Conference and Expo (ITEC)*, June 2016, pp. 1–5.

[3] C. Kaehler and G. Henneberger, "Transient 3-d fem computation of eddy-current losses in the rotor of a claw-pole alternator," *IEEE Transactions on Magnetics*, vol. 40, no. 2 , Part: 2, pp. 1362 – 1365, March 2004.

[4] R. Tittarelli, Y. L. Ménach, E. Creusé, S. Nicaise, F. Piriou, O. Moreau, and O. Boiteau, "Space-time residual-based a posteriori estimator for the a$-\varphi$ formulation in eddy current problems," *IEEE Transactions on Magnetics*, vol. 51, no. 3, pp. 1–5, March 2015.

[5] J. Gyselinck, P. Dular, C. Geuzaine, and W. Legros, "Harmonic-balance finite-element modeling of electromagnetic devices: a novel approach," *IEEE Transactions on Magnetics*, vol. 38, no. 2, pp. 521–524, Mar 2002.

[6] T. Hara, T. Naito, and J. Umoto, "Time-periodic finite element method for nonlinear diffusion equations," *IEEE Transactions on Magnetics*, vol. 21, no. 6, pp. 2261–2264, November 1985.

[7] G. Caron, T. Henneron, F. Piriou, and J. C. Mipo, "Time-periodicity condition of nonlinear magnetostatic problem coupled with electric circuit imposed by waveform relaxation method," *IEEE Transactions on Magnetics*, vol. 52, no. 3, pp. 1–4, March 2016.

[8] C. Emson and J. Simkin, "An optimal method for 3-d eddy currents," *IEEE Transactions on Magnetics*, vol. 19, no. 6, pp. 2450 – 2452, November 1983.

[9] T. W. Preston, A. B. J. Reece, and P. S. Sangha, "Induction motor analysis by time-stepping techniques," *IEEE Transactions on Magnetics*, vol. 24, no. 1, pp. 471–474, Jan 1988.

[10] A. Bossavit, "Whitney forms: a class of finite elements for three-dimensional computations in electromagnetism," *IEE Proceedings A - Physical Science, Measurement and Instrumentation, Management and Education - Reviews*, vol. 135, no. 8, pp. 493–500, November 1988.

[11] "Homard, a salome module for mesh adaptation," https://docs.salome-platform.org/latest/gui/HOMARD/en/.

[12] "Code avancé de recherche en modélisation électromagnńique," http://code-carmel.univ-lille1.fr.